

# Friction and Wear Studies on Nylon-6/SiO<sub>2</sub> Nanocomposites

Montserrat García,<sup>1</sup> Matthijn de Rooij,<sup>2</sup> Louis Winnubst,<sup>1</sup> Werner E. van Zyl,<sup>1\*</sup> Henk Verweij<sup>1†</sup>

<sup>1</sup>Laboratory for Inorganic Materials Science, Faculty of Science and Technology, MESA<sup>+</sup> Research Institute, University of Twente, P.O. Box 217, 7500 AE Enschede, The Netherlands

<sup>2</sup>Tribology Group, Faculty of Mechanical Engineering, University of Twente, P.O. Box 217, 7500 AE Enschede, The Netherlands

Received 15 April 2003; accepted 9 December 2003

**ABSTRACT:** Composites of nanometer-sized silica (SiO<sub>2</sub>) filler incorporated in nylon-6 polymer were prepared by compression molding. Their friction and wear properties were investigated on a pin on disk tribometer by running a flat pin of steel against a composite disc. The morphologies of the composites as well as of the wear track were observed by scanning electron microscopy (SEM). The addition of 2 wt % SiO<sub>2</sub> resulted in a friction reduction ( $\mu$ ) from 0.5 to 0.18 when compared with neat nylon-6. This low silica loading

led to a reduction in wear rate by a factor of 140, whereas the influence of higher silica loadings was less pronounced. The smooth morphology obtained after the wear test indicated the negligible contribution to friction of the pin to the nanocomposite. © 2004 Wiley Periodicals, Inc. *J Appl Polym Sci* 92: 1855–1862, 2004

**Key words:** nanocomposites; nylon-6/silica system; friction; wear

## INTRODUCTION

In recent years, there has been rapid growth in the use of thermoplastic polymers to replace metal components in wear-resistant applications.<sup>1</sup> Dry metal-polymer bearings are used for cost reduction and facile assembly in production. Because of their hardness, toughness, and friction properties, polyamides (PA) are used for gear and bearing materials.<sup>2</sup> For these applications, carbon, copper compounds (e.g., CuO), or glass fibers as filler components and poly(tetrafluoroethylene) (PTFE) or MoS<sub>2</sub> as solid lubricants have been added to PA.<sup>3–6</sup> The former improves mainly the mechanical strength and wear resistance of polymers, whereas the latter improves friction characteristics and contributes to the control of wear.<sup>1,7</sup>

Nylons are semicrystalline and their crystallinity can be modified by decreasing cooling rates during the thermal molding<sup>8</sup> and by the addition of a nucleating agent such as fumed silica or aluminum. However, high amounts of nucleating agents can cause brittleness or unwanted tribological properties in the materials.

The role of the filler component in influencing the wear behavior of polymers is not yet completely understood but plausible explanations have been provided.<sup>9,10</sup> The mechanical and/or chemical interaction between composite and counterface are believed to affect the wear process.<sup>11</sup> Sliding tests of a steel pin on polymer discs have shown that part of the polymer is transferred to the surface of the pin, producing shielding of the soft polymer surface from the hard metal asperities. The excellent heat-transfer characteristics of the metallic counterpart contribute to this film formation during frictional processes in almost all polymers with viscoelastic properties.<sup>6,12</sup> The wear of spherulitic nylon is preceded by interfacial frictional heating and subsequent removal of the material and transfer to the counterface as well. Therefore, the wear resistance of nylon is attributed to its ability to form thin films while sliding against a steel counterpart. A self-lubricating polymer-matrix material is used in the aviation and aerospace industry<sup>13</sup> because their coefficient of friction is low (typically between 0.1 and 0.5) compared to metal-to-metal contacts. Corresponding values of the dimensional wear coefficient ( $K_w$ ) are typically in the range of  $10^{-6}$  to  $10^{-3}$  mm<sup>3</sup> (Nm)<sup>-1</sup>. A wear rate of  $10^{-6}$  mm<sup>3</sup>/Nm is usually set as a limit above which a material is no longer considered wear-resistant. Thermoplastic polymer matrix composites are also used as coating materials for the bore of tubulars used as water injectors in the oil industry. Nylon-6 occupies a prominent position in the engineering thermoplastics because of its wide spectrum of properties, such as high crystallinity, high strength, and feasibility

Correspondence to: L. Winnubst (a.j.a.winnubst@utwente.nl).

\* Present address: Department of Chemistry and Biochemistry, Rand Afrikaans University, P.O. Box 524, Auckland Park 2006, South Africa.

† Present address: Department of Material Science and Engineering, The Ohio State University, Columbus, OH USA.

ity of fabrication and processing.<sup>14</sup> The tribological behavior of polyamide and their composites has been reported previously.<sup>6,15</sup> Polyamide has superior wear-resistance sliding against a steel counterface relative to other polymers. Factors that exert influence on friction and wear characteristics of polymer composites are the particle size, morphology, and concentration of the filler. If the particles are large and hard, they are readily pulled out of the matrix material and contribute to wear of the composites by their abrasive action and cause wear and damage of the counterpart material. For example, when fused silica and dolomite fillers with a particle size of 5 and 10  $\mu\text{m}$  were used in polymeric coatings, the filled nylon showed the worst abrasive wear resistance.<sup>16</sup> The fillers, rather than supporting the load, were pulled out, causing cracks in the material because of the poor bonding between filler and matrix material. The incorporation of filler to polymers has modified the coefficient of friction ( $\mu$ ) and/or wear rate ( $K_w$ ), although the detailed mechanism is still unclear.<sup>3-7</sup> By using nanoparticles, particle pull-out can be avoided because better adhesion between polymer and filler is expected because of the high surface area of the nanoparticle.

Silica nanoparticles are currently used for the enhancement of the mechanical properties in PA-6.<sup>17</sup> In this study, the effect of nanosilica addition in nylon-6 on the tribological performance was investigated. Cooling rates were kept constant for the consolidation of the nanocomposites. The material's microstructure and dispersion of the nanocomposite were studied by scanning electron microscopy (SEM).

## EXPERIMENTAL

### Synthesis of nanocomposites

Nylon-6 was obtained from Sigma-Aldrich (The Netherlands). Two extreme values of silica particles were studied: 2 and 14 wt % because at 2 wt % particles are homogeneously dispersed and at 14 wt % particles are more likely to be aggregated. For the preparation of 2 wt % nanocomposites (2NS), silica nanoparticles were synthesized in-house. Tetraethylorthosilicate (TEOS, 21 mL) (Aldrich, The Netherlands) was slowly added to 21 mL of dry ethanol (1 : 1 vol/vol). The mixture was stirred and 8 mL of 1M  $\text{HNO}_3$  was added. The sample was heated to 60°C for 3 h together with 3 mL of deionized water and then placed in an ice-bath. The silica sol (5 mL) was dispersed in EtOH (90 mL) and kept in the refrigerator for 1 week.<sup>18</sup> The resulting particle size of the spheres was  $\leq 20$  nm in diameter. For the nanocomposite with 14 wt % of silica loadings (14NS), the silica sol SNOWTEX® (Nissan Chemical, Japan), with a particle size of 10–20 nm, was used. The preparation of the nanocomposite has been described elsewhere.<sup>19</sup> Nylon films were produced by drawing a

steel knife over a pretreated glass containing a solution of the polymer in formic acid at a rate of 1 mm  $\text{min}^{-1}$  by using Doctor Blade™ equipment. Films produced were 0.1- to 0.5-mm-thick. The composite was left overnight in inert atmosphere and a film coating of 1 mm formed on the glass. During the elaboration of the nanocomposite, temperatures of 80 and 250°C were used in the vacuum oven and compression molding, respectively (*vide infra*). The formic acid, water, and/or ethanol are expected to evaporate during the production of the sample. The final products comprise a pure system of nylon-6 and silica nanoparticles.

### Compression molding of the nanocomposites

Prior to tribological measurements, the film-cast nanocomposites were compression molded into sheets measuring  $19 \times 5.5$  cm<sup>2</sup> and a thickness of 1 mm at 250–260°C. Compression was performed in three steps, as follows: 2 min at 5 MPa, 3 min at 10 MPa, and 5 min at 20 MPa at 250°C, and subsequently, the samples were cooled to room temperature.

### Characterization

Wide-angle X-ray diffraction (WAXD) patterns at room temperature of the nylon-6 with nanosilica were obtained. Partially crystalline nylon consisted of a broad amorphous halo on which the peaks from the crystalline regions were superimposed. Thus, the normalized area of the crystalline peaks could be used to obtain the degree of crystallinity.<sup>7</sup> Analysis of the crystallinity was performed by using a Philips PW3710 diffractometer. Microstructures and wear tracks were characterized by means of SEM by using a Hitachi S800 with an in-lens detector. To determine phase distribution and the presence of impurities, energy-disperse X-ray analysis (EDX, KeveX) was used coupled with SEM. Quantitative XRF was used to determine the amount (as wt %) of silica present in each sample by utilizing a Philips PW 1480/10 fluorometer (Eindhoven, The Netherlands).<sup>20</sup> The composition of the outermost atomic layer of the nanocomposites was measured by low-energy ion scattering (LEIS).<sup>21,22</sup> The samples were first bombarded with low-energy (noble gas) ions by using a 3-keV  $^3\text{He}^+$  beam. During the measurements, an area of 1.4 mm<sup>2</sup> was analyzed and only about a 0.3 atomic layer was removed. Further analysis of the surface was done with XPS spectra taken with a Quantum 2000 Scanning Esca Probe of Physical Electronics. The AlK $\alpha$  X-ray beam had a power of 25 W and the analysis area was  $1000 \times 500$   $\mu\text{m}$ . For calibration of the spectra, the C1s line of aliphatic carbon (284.8 eV) was chosen as reference. LEIS study of one sample was used to verify

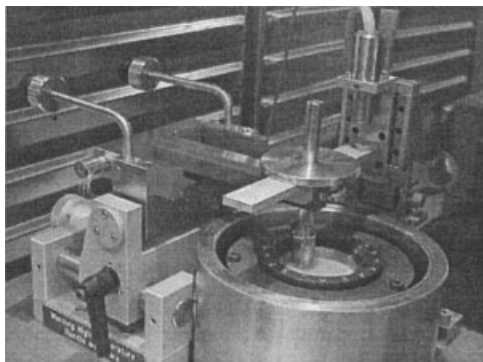


Figure 1 The test set-up.

the silica particles of the outermost atomic layer on the nanocomposites.

### Tribological conditions

The compression-molded polymers were cut into discs with a diameter of  $\sim 40$  mm and thickness between 0.9 and 1.07 mm. The disc surface roughness varies from  $R_a = 0.5$  to  $1.4 \mu\text{m}$ . The roughness of the pin was  $R_a = 0.15 \mu\text{m}$ . Dry sliding-wear tests were performed with a pin-on-disc tribometer (CSEM, Neuchatel, Switzerland), placed in a climate chamber (Heraeus, HC4057, Balingen, Germany) at  $23^\circ\text{C}$  and 40% relative humidity. A picture of the test set-up is shown in Figure 1 and consisted of a flat round steel pin 100McCrW4 sliding against a rotating polymer sample. The sliding velocity for the nanocomposites was set at 0.1 m/s to avoid the occurrence of a high PV (applied pressure  $\times$  sliding velocity) value for nylon and of possible thermally induced fracturing. The load used was 1N and the mean initial contact pressure was 0.7 MPa with a pin of 1.3 mm. The resulting PV was  $75,339\text{N/m s}$ . The sliding distance of the tests was adapted for each specific measurement to obtain significant wear and to detect possible fatigue and was set at a distance of 10 km. The coefficient of friction was measured on-line by monitoring the ratio between the measured shear force and the applied normal force through measurement of the deflection of the pin-arm (lever) with two inductors. The wear track depth after the test was measured with a Micromap 512 opto-profiler. The measurements have been duplicated.

## RESULTS

### Sample characteristics

WAXD patterns of the nylon-6 with nanosilica at room temperature were obtained. Two strong peaks located at  $2\theta$  values of  $21^\circ$  and  $23^\circ$  were characteristic of the  $\alpha$ -form of nylon-6 crystal, which was assigned as the

TABLE I  
Degree of Crystallinity of the Composites

Sample	$2\theta$	$\beta_m$ measured FWHM	$X_c$ (%)
PA6	23.54	1.31	33
2NS	23.71	1.17	39
14NS	23.76	1.22	36

(200) and (002), (202) reflections. The degree of crystallinity of the  $\alpha$ -phase of nylon-6 was obtained from the multiplex resolution method.<sup>23</sup> Table I shows the intensities and assignments of the pure PA-6, PA compression molded with 2 wt % of nanosilica (2NS) filler, and PA compression molded with 14 wt % of silica (14NS). The degrees of crystallinity of the samples were 33, 39, and 36%, respectively.

The results for the LEIS measurements of the 14NS nanocomposite before the friction experiments are shown in Figure 2. The Si, O, C, and Cl peaks were clearly observed. The value of the Si—O ratio corresponded with the ratio of a pure silica sample, indicating the presence of SiO<sub>2</sub> nanoparticles on the surface. The silica particles in 2NS were well dispersed and had an average particle size of  $\leq 20$  nm, as seen by SEM (Fig. 3). The picture showed individual nonaggregated white particles characterized by EDX as SiO<sub>2</sub>. This was in agreement with the LEIS study, which showed that silica could be detected in the outermost atomic layer of the composite.

### Tribological tests

Table II shows the coefficient of friction ( $\mu$ ) and specific wear rate ( $K_w$ ) of the PA6, 2NS, 14NS nanocomposites and the correspondent  $\mu$  measurements against sliding distance are shown in Figure 4. Pure nylon showed a  $\mu$  of 0.18 at the beginning of the friction measurements. During the test, the  $\mu$  was gradually elevated up to a steady state of  $\mu = 0.45$ . At

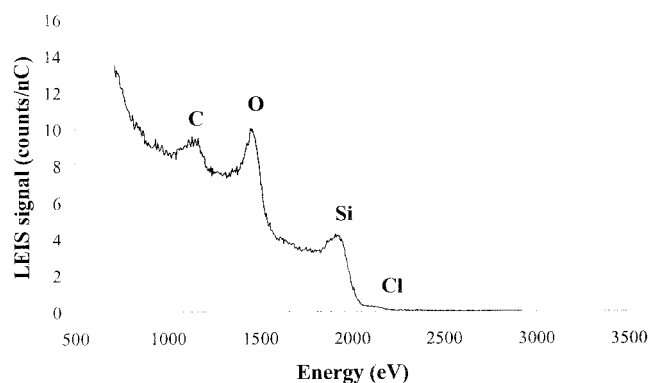
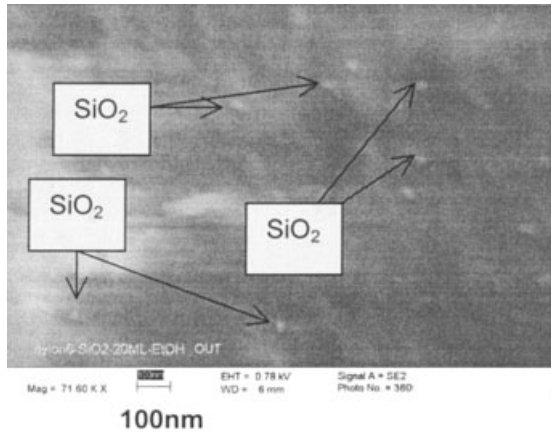


Figure 2 LEIS results of the 14 NS nanocomposite before testing.



**Figure 3** Silica nanoparticles dispersed in the polymer matrix (2NS).

filler loadings of 2 wt %, the starting  $\mu$  was 0.14. This nanocomposite rapidly reached a steady value of  $\mu = 0.18$ . The addition of 14 wt % of silica in the PA-6 resulted in an initial  $\mu$  of 0.11. After 0.1 km, a transient period resulted in  $\mu = 0.2$ , whereas after 1 km, a building up of  $\mu$  was again observed up to almost the same steady-state value of the neat polymer (0.40). The opto-profiler of the resulting wear track in the 14NS is shown in Figure 5. As seen from this figure, higher volume was lost close to the middle of the track.

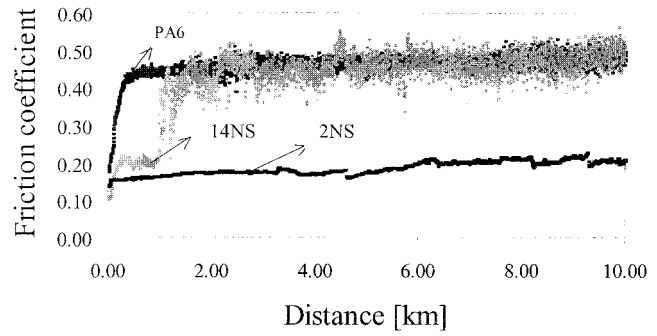
It was observed that the coefficient of friction for 2 wt % of SiO<sub>2</sub>-filled composite was lower than that of unfilled nylon-6. Addition of 14 wt % of SiO<sub>2</sub> resulted in a coefficient of friction value ( $\mu$ ) slightly lower than pure nylon-6 after a few kilometers of wear track. Therefore, the 2NS composite had a lower wear rate and a lower coefficient of friction when compared to PA6 and 14NS.

Figure 6 shows the worn disc surface after the test of the 2NS nanocomposite. An overview of the 2NS nanocomposite wear track is shown in Figure 6(a). A detailed photograph of the edge of the 2NS wear track is shown in Figure 6(b). The micrograph showed different surface microstructure when compared the wear track with the area outside. A higher magnification as given in Figure 6(c) showed a patchy layer

**TABLE II**  
Wear Rate and Coefficients of Friction of PA6 (C) Nanocomposites

Silica (wt%)	Friction coefficient ( $\mu$ )	Wear rate [mm <sup>3</sup> /Nm] ( $K_w$ )
0	0.45	$5.29 \times 10^{-5}$
2	0.20	$2.0 \times 10^{-7}$
14	0.40	$2.81 \times 10^{-5}$

Velocity = 0.1 m/s; Load = 1N, Distance of sliding 10 km.



**Figure 4** Plot of coefficients of friction ( $\mu$ ) against sliding distance for PA-6 and nanocomposites on steel counterface. Velocity = 0.1 m<sup>-1</sup>; load = 1N.

formed after the test, whereas in Figure 6(d), a smooth character is seen along the track.

SEM pictures of the 14NS nanocomposite are shown in Figure 7. The edge of the wear track at these silica loadings is seen in Figure 7(a). Irregular patches were formed along the wear track [Fig. 7(b)]. At higher magnifications, a rough surface topography was observed and groove formation with particle dislodging during sliding was evident [Fig. 7(c)]. The surface also showed accumulation of worn material in the wear track in the form of lumps [Fig. 7(d)].

SEM pictures of the pin of the 14NS were taken to verify film formation on the counterface, as shown in Figure 8(a). The surface seemed to be covered with worn material that has probably been back-transferred from the counterface to the pin surface. At higher magnifications, compacted long patches were also seen [Fig. 8(b)]. After the wear test, good dispersion of the nanoparticles in the polymer was seen on the pin counterface, as indicated in Figure 8(c).

**DISCUSSION**

The XRD results indicated the positive effect of the filler on nucleation. As indicated in Table I, the degree of crystallinity slightly increased with 2NS composite when compared with pure nylon-6. As a semicrystalline polymer, nylon-6 is regarded as a two-phase sys-

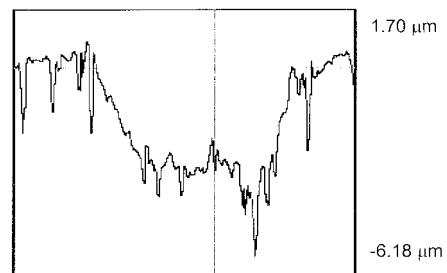


**Figure 5** Opto-profiler of the wear track of the filled nylon (14 wt %). Length: 1741  $\mu$ m; area: 1741  $\times$  1346  $\mu$ m.

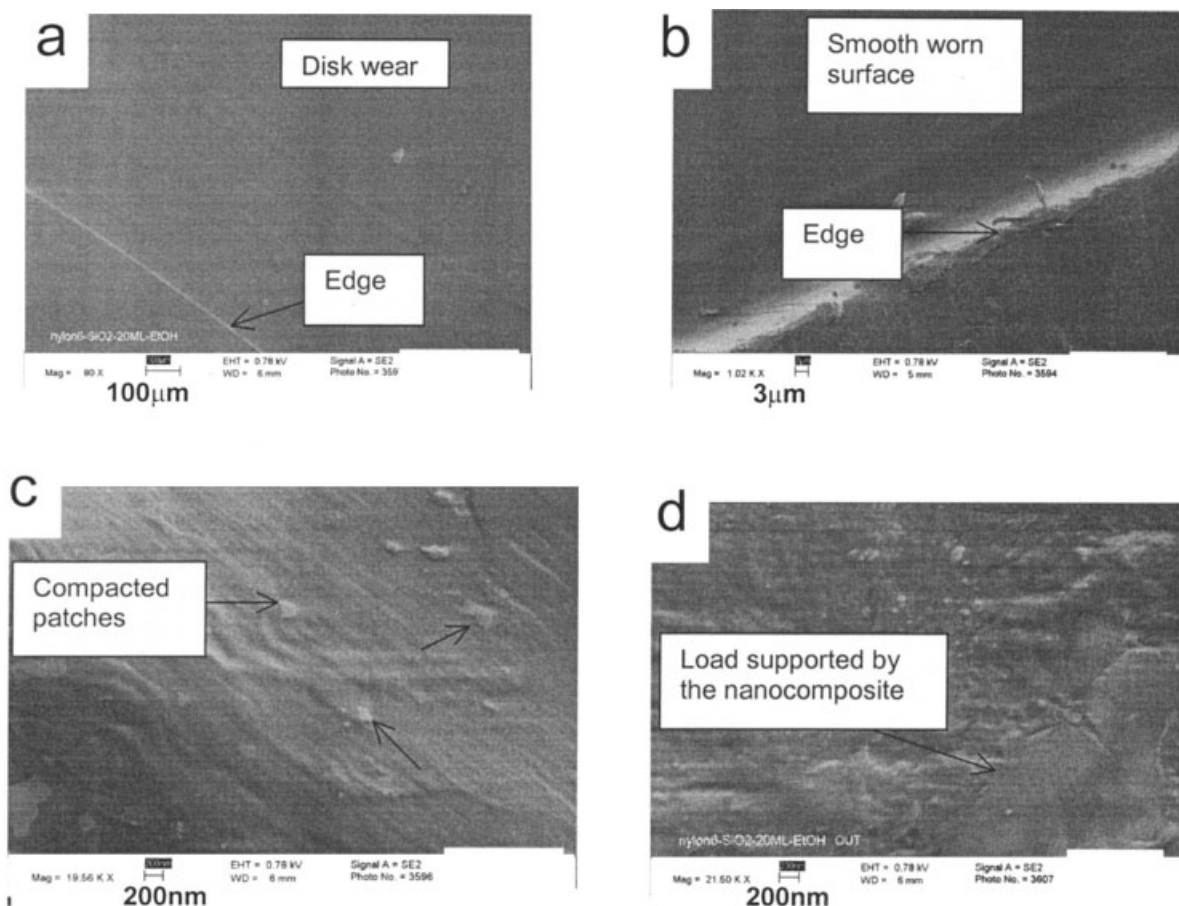


Figure 6 Wear track of 2NS nanocomposite as shown by SEM.

tem consisting of crystalline and amorphous regions. The chain segments existed as folded chain lamellae organized into spherulites. Crystalline structures have higher density than amorphous structures because of the highly ordered packing. More energy is required to damage this orderly packed dense crystalline material than for disrupting the loosely packed amorphous materials.<sup>24</sup> Cartledge<sup>8</sup> demonstrated that higher crystallinity (varying cooling rates) results in a hard composite with high wear resistance.

### Friction and wear

All quantitative discussions of friction depend critically on the experimental conditions under which it was measured. The neat polymer showed an initial coefficient of friction of 0.2, which gradually elevated up to a steady state of 0.45 (Fig. 4). This study showed that the silica nanoparticles were effective in reducing the coefficient of friction ( $\mu$ ) and wear rate ( $K_w$ ) of PA6 when added in an amount of 2 wt % (Table II). The plate abraded the pin slightly; this process increased the coefficient of friction at the start of the test. After this transient period, the plate reduced the surface roughness of the polymer and also provided a cleaner

surface. Both factors tended to avoid the increase in the coefficient of friction. The resulting  $\mu$  and  $K_w$  for the 2NS composite was lower than for the 14NS composite, which showed during the first kilometer a  $\mu$  of 0.20. After 1.32 km, the  $\mu$  of 14NS varied until a steady coefficient of friction comparable to that of unfilled nylon-6 ( $\mu = 4.0$ ).

A transfer of polymer to the metal surface initiated by adhesion between the two materials, during sliding, contributed to shear in the subsurface region of the contact. Even in static contact, this transfer was reported in a polymer such as PTFE.<sup>9</sup>

In Figure 9, a schematic illustration of the friction model for 2NS and 14NS during sliding is shown. In the initial stage of sliding (first kilometer), there was an intimate contact between pin and disc [Fig. 9(a, b)]. Further sliding involved the transfer of polymer to the harder metallic counterface caused by electrostatic forces (e.g., van der Waals) or tribochemical reactions on the surface [Fig. 9(c, d)]. It was believed that the nanosilica particles in the composite improved the adhesion to the counterface, resulting in a lowered wear rate by a factor of  $10^2$  in the case of 2NS. The bonding between polymer and counterface was in this case stronger. The contact of the nanocomposite with

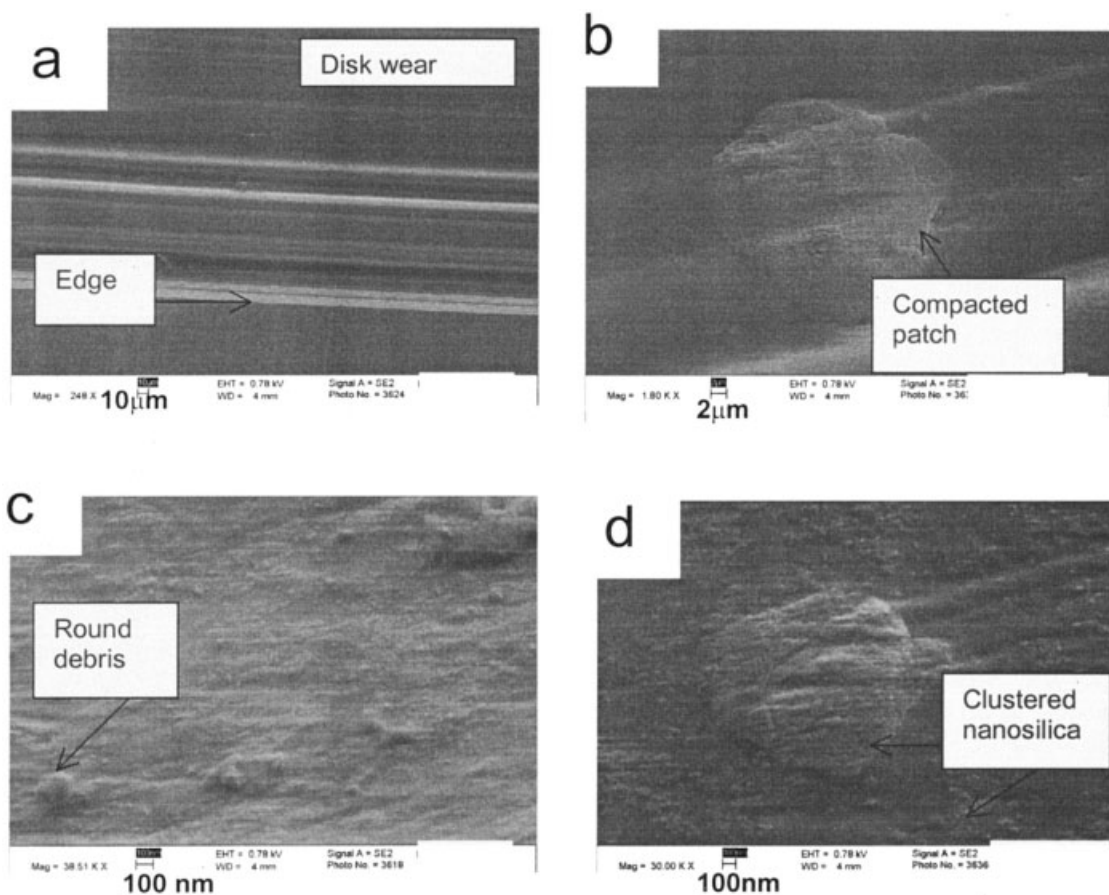


Figure 7 Wear track of the 14NS nanocomposite.

the pin led to a layer formation by material removal from the disk to the counterface (*vide infra*), adhesive wear being the most important mechanism for this layer formation.

The layered-film formation observed on the pin in the 14NS experiment as visible in Figure 8(a) was explained as follows: Part of the nanocomposite was transferred to the steel counterface and upon sliding a secondary contact occurred. After consecutive sliding, the material was transferred to the counterface filling the uneven surface of the pin [Fig. 9(c, d)]. In the case of 14NS, repeated movement over the pin led to progressive build up of a transferred layer, as seen in Figure 8(b). The detachment of material from the disc to the pin was aided by the nanoparticles, as seen at higher magnification in Figure 8(c). This is schematically represented in Figure 9(f).

The smooth and compacted patches observed in Figure 6(c) suggested that in the 2NS case, the material was retransferred to the disc in patches, supporting the total load of the pin during sliding. This process led to a deformed material as seen in Figure 6(d). Upon consecutive contact, the migration of the nanocomposite took place forming a film on the pin as schematically illustrated in Figure 9(e). The difference

in frictional behavior of 2NS and 14NS composite was then attributed to the difference in composite-counterface interaction.

SEM photographs from the edge of the 2NS material [Fig. 6(b)] suggested that the smooth surface observed on the wear track was due to the formation of a protective film. It was believed that for 2NS a uniform layer was formed on both faces and that during sliding the surface molecules of the polymer were highly oriented in the direction of sliding. The layer adhered well to the pin, and further sliding occurred between the surface of the bulk polymer, which contained similarly oriented molecules than the transfer film on the counterface [Fig. 9(g)].

On the contrary, the 14NS involved peeling-off of material from the transfer film followed by rolling, as seen in Figure 7(c). The difference in coefficient of friction can be related to a higher degree of interfacial wear of the disc and the counterface. Higher amounts of silica particles in PA-6 filled the rough parts of the counterparts in less time than in 2NS. Even though a layer in 14NS was formed more rapidly than in 2NS, this layer eventually became detached, forming round debris asperities, as illustrated in Figure 9(f). Under these conditions, the polymer was transferred to the

counterface in regular lumps [Fig. 7(c)] and patches 0.1 to 10 μm thick [Fig. 7(d)].

The rate of wear appeared to be dictated by the rate of removal of the transfer film from the counterface, rather than by the rate of polymer transfer into the film.

To study possible chemical changes during sliding, XPS experiments on the pin and transfer material was performed. Fe<sub>2</sub>O<sub>3</sub> formation was seen as caused by the oxidation of steel. Except for the Fe<sub>2</sub>O<sub>3</sub>, no chemical

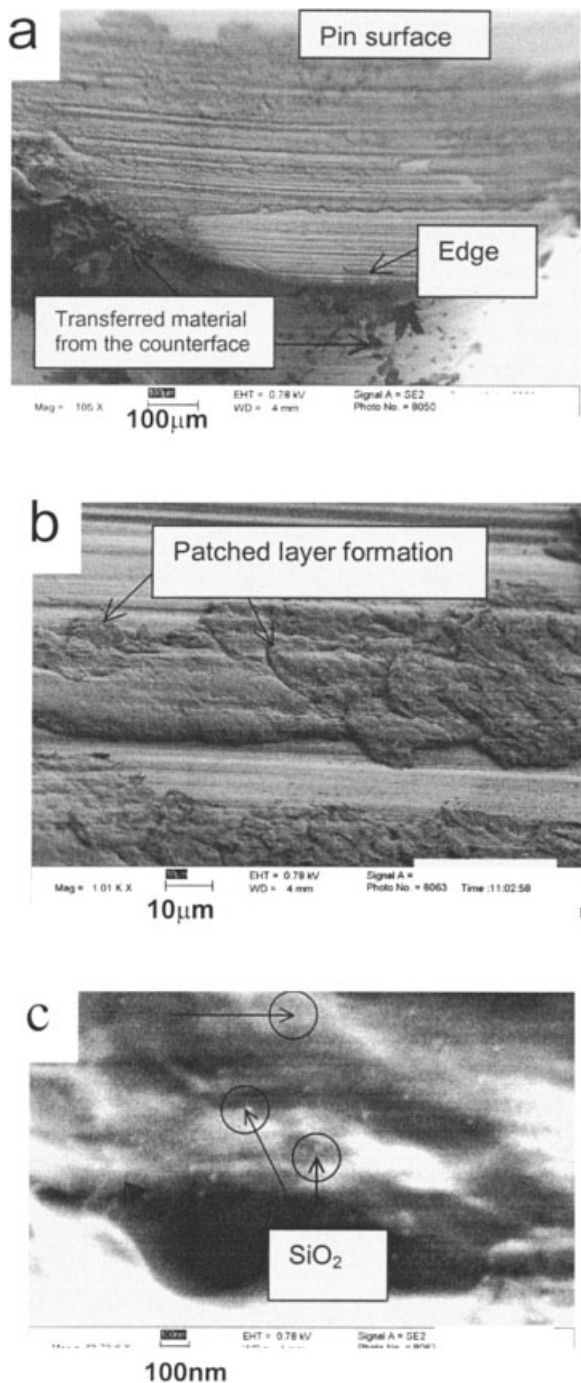


Figure 8 Pin counterface of 14NS nanocomposite.

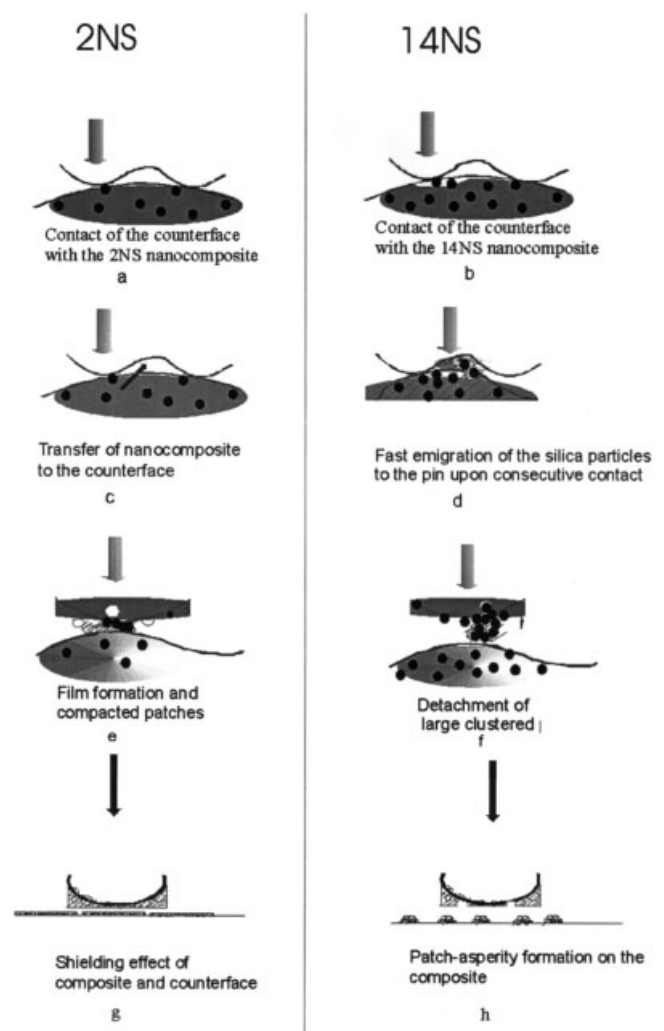


Figure 9 Scheme and proposed mechanism of the film formation when using 2 wt % (left) and 14 wt % silica nanoparticles (right).

change occurred in the process of nylon-6/nanosilica sliding against the steel disk.

### CONCLUSION

The addition of a second phase was one of the methods used to improve the tribological properties of the thermoplastic PA6 (such as coefficient of friction and wear rate). The addition of 2 wt % nanosilica particles improved the coefficient of friction and wear resistance of nylon-6 composites. Smooth surfaces were obtained in the nanocomposites, indicating a well-functioning tribological system. A transfer film on the steel pin was developed, caused by adhesion and interlocking of fragments of material into metal asperities. Wear depended upon the adhesion of the transfer film to the counterface, and the protection of polymer surface from metal asperities by transfer film. A systematic study is necessary to find out the threshold

value of filler concentration where the nanocomposites start showing a lower coefficient of friction.

The authors acknowledge D. Schipper for very useful discussions and E. de Vries for performing the tribological experiments. M. Viitanen from Calipso, Eindhoven is acknowledged for the LEIS experiments. M. Smithers is thanked for the SEM pictures; A. van der Berg is thanked for the XPS measurements (MESA<sup>+</sup> Institute), and H. Koster is thanked for the XRD measurements.

## References

1. Hironaka, S. *Jpn J Tribol* 1997, 42, 931.
2. Theberge, J. E. *Proc Anniv SPI (Soc Plast Ind), Reinf Div*, 25th, 2-D, 1–12, 1970.
3. Bahadur, S.; Gong, D.; Andereg, J. W. *Wear* 1992, 154, 207.
4. Bahadur, S.; Polineni, V. K. *Wear* 1996, 200, 95.
5. Bahadur, S.; Gong, D.; Andereg, J. W. *Wear* 1993, 160, 131.
6. Tanaka, K. *Wear* 1982, 75, 183.
7. Kohan, M. I. *Nylon Plastics Handbook*; Hanser: New York, 1995.
8. Cartledge, H. C. Y. *J Mater Sci* 2002, 37, 3005.
9. Bahadur, S. *Wear* 2000, 245, 92.
10. Martin, J. M.; Grossiord, C.; Le Mogne, T. *Wear* 2000, 245, 107.
11. Jintang, G. *Wear* 2000, 245, 100.
12. Tanaka, K.; Miyata, T. *Wear* 1977, 41, 383.
13. Jintang, G. *Wear* 2000, 245, 100.
14. Palabiyik, M.; Bahadur, S. *Wear* 2000, 246, 149.
15. Watanabe, M.; Yamaguchi, H. *Wear* 1986, 110, 379.
16. Xu, Y. M.; Mellor, B. G. *Wear* 2001, 251, 1522.
17. Reynaud, E.; Jouen, T.; Gauthier, C.; Vigier, G.; Varlet, J. *Polymer* 2001, 42, 8759.
18. Bernards, T. N. M.; van Bommel, M. J.; Boonstra, H. A. *J Non-Cryst Solids* 1991, 134, 1.
19. van Zyl, W. E.; Garcia, M.; Schrauwen, B. A. G.; Kooi, B. De Hosson, J. Th. *Macromol Mater Eng* 2002, 287, 106.
20. Bekkers, M. H. J.; van Sprang, H. A. *X-ray Spectrom* 1997, 26, 122.
21. Maas, A. J. H.; Viitanen, M. M.; Brongersma, H. H. *Surf Interface Anal* 2000, 30, 3.
22. van Welzenis, R. G. *Ionics* 1999, 5, 13.
23. Mo, Z.; Zhang, H. *JMS Rev Macromol Chem Phys C* 1995, 35 (4), 555.
24. Hutchings, I. M. *Tribology*; Edward Arnold: London, 1992.